



Material classification technology based on Convolutional neural networks

Dailin Li^{*a}, Guilei Li^a, Baojun Wei^a, Dan Yang^a, Ning Wang^a, Huafeng Zhu^a, Hao Ni^a

^aCollege of Science, China University of Petroleum (East China), Qingdao 266580, China

*Li Dailin, E-mail: qd_ldl@upc.edu.cn

ABSTRACT

The contact measurement techniques are typically used in the field of object material classification. It has a lot of disadvantages, such as the complex operation and time-consuming. In this paper, a new non-contact object material identification method based on Convolutional neural networks (CNNs) and polarization imaging is proposed. Firstly, the relationship between the complex refractive index of object and the polarization information is simulated, and then the structure of the CNNs is constructed according to the specific conditions of the polarization imaging system. The accuracy of the identification method is measured by repeated test using 7 materials. The experimental results show that the CNNs model can quickly realize the object material classification with the polarization images, and the classification accuracy is above 92%.

Keywords: Material classification; Convolutional neural networks; Polarization imaging; HSV color model

1. INTRODUCTION

Material classification is an important task in the fields of industrial automation , disease-detection and agricultural seed sifting, as it provides important information for scene understanding of computer vision. With the fast development of Chinese economy, material classification technology is also developing rapidly.

In the present study, the object recognition and material classification technology with the image information is very mature ^[1-3]. This is only an application of the light intensity information, but the polarization information contained in the image is not utilized. Polarization imaging technology can effectively improve the quality of imaging by utilizing the polarization characteristics of scattered light. In recent years, it has played an important role in the field of material recognition ^[4], medical detection ^[5-6], image processing ^[7-8], target detection ^[9-10] and other fields. Compared with the traditional imaging technology, the polarization information can not be directly recorded by the human eyes or the camera, and it needs to be extracted by image processing. The polarization state of the light varies when the light reflects from different objects, so the polarization imaging technology can more fully characterize the object information.

Convolutional Neural Networks (CNNs) have been established as an effective class of models for image detection and recognition. It has the characteristics of intelligence, high stability and high accuracy, which have been shown to learn powerful and interpretable image features: such as font, expression or face recognition, crop screening and so on ^[11-14].

Encouraged by positive results above, we propose an object material identification method based on CNNs and polarization imaging technology in this paper. The variations of polarization was calculated with image processing algorithm, and the polarization information was visualized through HSV color space ^[15], finally the classification of object materials was realized by using CNNs model constructed according to the specific conditions.

2. MATERIAL IDENTIFICATION THEORY FOUNDATION

2.1 Principle of polarization reflection

The polarization of light is a property that describes the preferential orientation of oscillation of its electromagnetic field. In monochromatic light, it is usually described using the Stokes column matrix, and the Stokes vector for elliptically polarized light is as follows

$$S = (I, Q, U, V)^T$$

$$\begin{bmatrix} I \\ Q \\ U \\ V \end{bmatrix} = \begin{bmatrix} E_{ox}^2 + E_{oy}^2 \\ E_{ox}^2 - E_{oy}^2 \\ 2E_{ox}E_{oy}\cos\delta \\ 2E_{ox}E_{oy}\sin\delta \end{bmatrix} = \begin{bmatrix} I_x + I_y \\ I_x - I_y \\ 2I_{45} - I_0 - I_{90} \\ I_R - I_L \end{bmatrix} \quad (1)$$

Where I represents the total intensity of the radiation, Q represents the linearly polarized light component in the x-axis direction, U represents the linearly polarized light component in the 45° angle with the x-axis, and V represents the dominant left-handed or right-handed circularly polarized light. The polarization of light reflected from a surface can be measured by mounting a linear polarizer in front of the camera.

After the laser illuminates the object, the Stokes parameter of the reflected light is linearly related to the incident beam and it can be expressed as ^[16]:

$$S_{out} = M \cdot S_{in}$$

$$\begin{bmatrix} I' \\ Q' \\ U' \\ V' \end{bmatrix} = \begin{bmatrix} m_{00}m_{01}m_{02}m_{03} \\ m_{10}m_{11}m_{12}m_{13} \\ m_{20}m_{21}m_{22}m_{23} \\ m_{30}m_{31}m_{32}m_{33} \end{bmatrix} \begin{bmatrix} I \\ Q \\ U \\ V \end{bmatrix} \quad (2)$$

Where M is the Miller matrix of the polarizing device. The difference between the reflected left-handed and right-handed circularly polarized light is negligible, so V=0 in the algorithm. Therefore, the polarization state of the reflected light of the object can be obtained by measuring three parameters of I, Q, and U. The polarization degree and polarization angle of the images can be obtained by taking different images at three or more degrees. So the stokes vector of reflected light can be expressed as:

$$S_{out} = \begin{bmatrix} I \\ Q \\ U \end{bmatrix} = \begin{bmatrix} I_0 + I_{90} \\ I_0 - I_{90} \\ 2I_{45} - I_0 - I_{90} \end{bmatrix} \quad (3)$$

Where I_0 , I_{45} , I_{90} are linearly polarized light images with angles of 0° , 45° , and 90° , respectively, with respect to the reference axis.

The polarization degree and polarization azimuth of the reflected light can be obtained by the three parameters in the above equation:

$$p = \frac{\sqrt{Q^2 + U^2 + V^2}}{I} \quad (4)$$

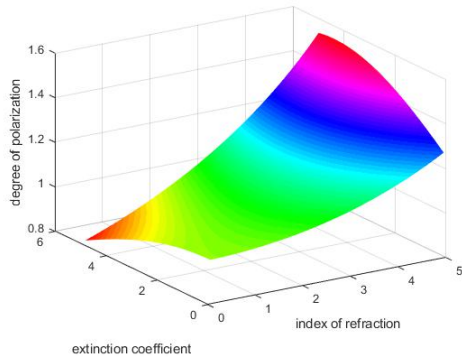
$$\theta = \frac{1}{2} \tan^{-1} \left(\frac{U}{Q} \right) \quad (5)$$

When an incident beam interacting with a material, the emerging beam will carry some information of the material. Since the characterization of the polarized image vary with the material types, so the material of the object can be characterized by the polarization degree and the polarization azimuth of the reflected light.

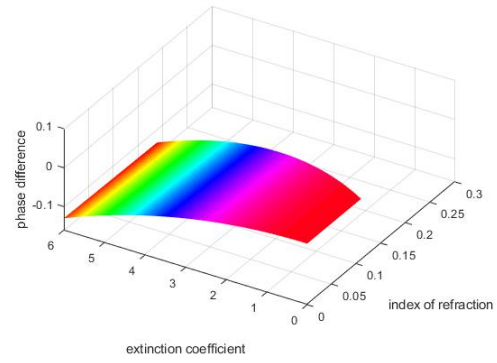
In order to improve the classification accuracy of polarization, it is mapped into HSV (Hue, Saturation, Value) color space, which is closer to human visual experience than the traditional RGB color model. The degree of polarization p and polarization azimuth θ correspond to H, S, so that the polarization information contained in the reflected light of the object can be visualized.

2.2 Matlab numerical simulation

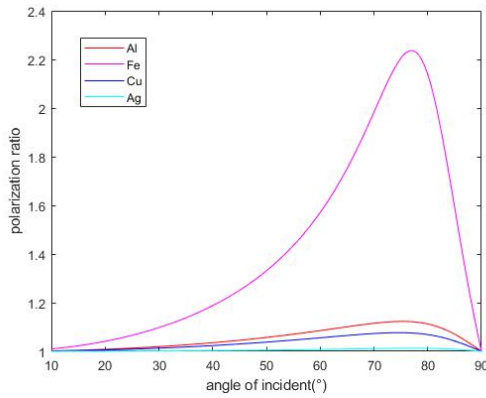
Every kind of object has its own unique refractive index and extinction coefficient, the polarization information of reflected light is different too. The Matlab software was used to simulate the interaction between light and matter with a wavelength of 632 nm, as shown in Figure 1. The change in the polarization state is expressed by the polarization ratio, that is, the intensity ratio of the light that vibrates in the vertical direction and the horizontal direction. The change in deflection angle is represented by the phase difference.



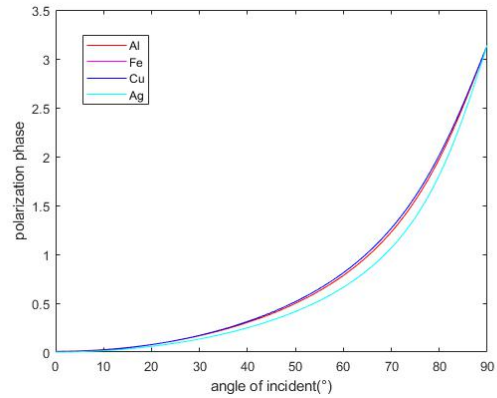
(a) The degree of polarization varies with refractive index and extinction coefficient



(b) Phase difference with polarization ratio as a function of refractive index and extinction coefficient



(c) Polarization ratio as a function of incident angle



(d) Phase difference as a function of incident angle

Fig. 1 Polarization information changes with parameters

Fig. 1(a)-(b) show the relationship between the polarization information and the complex refractive index (refractive index and the extinction coefficient) when the incident angle is 60° . As shown above, there is a one-to-one correspondence between the polarization information and the properties of a material.

Various metals such as Al, Fe, Cu and Ag were used in the simulation. In Fig. 1(c)-(d), the polarization ratio of the reflected light does change with the incident angle. The maximum value in curve of Fe is much larger than those one of Al, Cu and Ag. But the polarization ratio difference of Al, Cu and Ag is small, and phase difference curves of the four metals almost

equal to each other. When the parameters of polarization degree and the polarization angle are mapped into the HSV color space, they will have the nearly same color.

The ability that people can identify and differentiate the difference of confusable color is very limited, a method to recognize colors based on CNNs is proposed, which can replace human visual observation.

2.3 Convolutional neural networks

CNNs use relatively little pre-processing compared to other image classification algorithms. CNNs consist of an input and an output layer, as well as multiple hidden layers. The hidden layers of CNNs typically consist of convolutional layers, pooling layers, fully connected layers and normalization layers.

The construction of network structure needs the guidance of experimental data. Therefore, it is necessary to design specific CNNs according to the specific conditions of the experiment [17-18]. In order to recognize the slight difference of HSV color between different materials, a CNNs model was constructed. The constructed is shown in Figure 2.

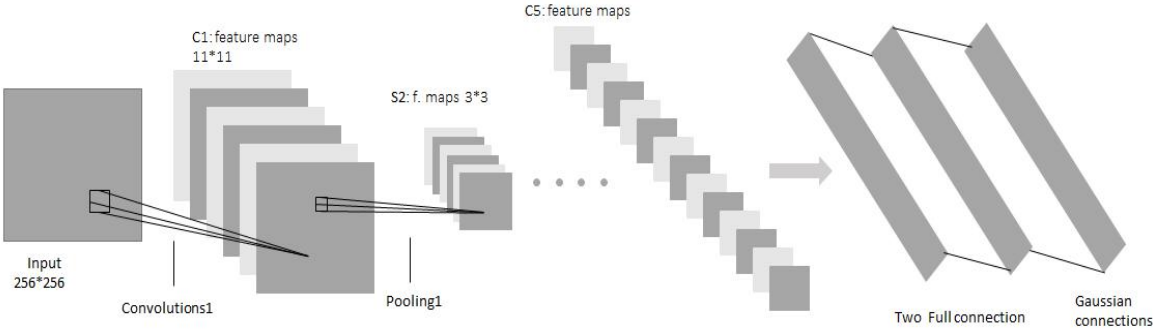


Fig. 2 CNNs structure diagram

The CNNs structure has a total of eight layers, including five layers of convolutional layers, two fully connected layers and one output classification layer. The first two convolutional layers are connected to the ReLU layer, the pooling layer and the local response normalization layer. The remaining convolutional layers are connected to the ReLU layer, the fifth convolutional layer is connected to the two fully connected layers after the pooling layer, and finally the data is imported into the classifier. The softmax classifier is used to calculate the probability of the category. In order to avoid over-fitting problems in the network, the

Dropout layer is added after the full connection layer, which can randomly make the weights of some hidden layer nodes of the networks.

The ReLU activation function is used in the networks, and its function formula is as follows:

$$g(x) = \max(0, x) \quad (6)$$

Its function graph is:

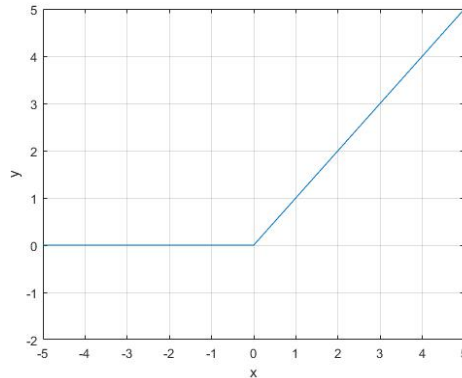


Fig. 3 ReLU activation function

Compared with the traditional activation function, ReLU is nonlinear and unsaturated. When the training gradient decreases, the ReLU has a faster convergence rate and better ability to characterize the transmission mechanism of biological neural network. ReLU can effectively alleviate the problem of gradient disappearance.

The number of convolution kernels is the number of feature maps. The number and size of convolution kernels will affect the recognition result. If the number of convolution kernels is too small, the recognition accuracy will be too low. On the contrary, it will extract too much useless information, which will greatly reduce the operation speed and may also cause network model over-fitting. The number of convolution kernels in this model is set to 96, the size is 11×11 , and the step size is 4. The CNNs extracts features and learns the characteristics from the input image, and the material classification is realized with the trained CNNs.

3. UNDERWATER MATERIAL IDENTIFICATION SCHEME DESIGN

3.1 Experiment process

The experiment process consists of three parts, namely information collection, image processing, sample training and testing. The main process of the design scheme is shown in the figure below.

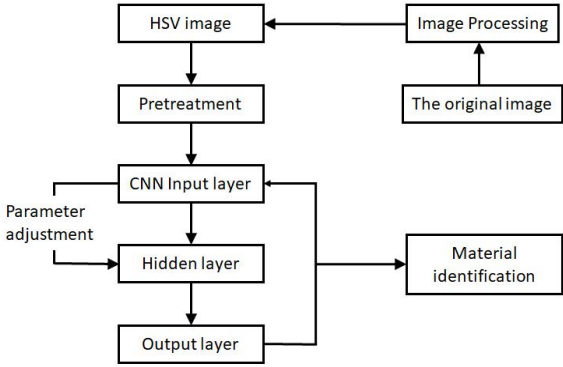


Fig. 4 flow chart

Firstly, the original polarization images of a material were collected with polarized light imaging system, and then were transformed into HSV images through digital image processing. These images were served as training samples for the network model, then a database of colors was built for each material based on the above information. With the Caffe framework, the CPU of the computer was used as a processor to train the HSV image samples of various materials. After the features extracted and learned process was done, a material recognition network model was constructed. Finally, the obtained model was used to test the sample to complete the material identification of the object.

3.2 Polarized light imaging system

The experimental setup for image acquisition is shown in Figure 5.

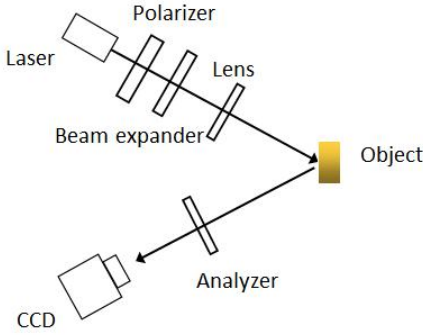


Fig. 5 Polarization imaging system diagram

The source used was a linearly polarized monochromatic laser with a wavelength of 632 nm, a polarizer was placed behind the laser, and the transmission direction was the same as the polarization direction of the laser light. Then, the emitted light was collimated and expanded by the beam expander and lens. The reflected light of the object was detected by the analyzer. Finally, the image was collected by the CCD camera. The main transmission direction of the polarizer remains the same, by rotating the analyzer, three original images are collected at 0° , 45° , and 90° with respect to a reference axis.

3.3 Collect training samples

The polarized imaging system was used to image the objects of different materials. Three original images of Zn with polarization angles of 0° , 45° and 90° were recorded by the CCD, as shown in Figure 6.

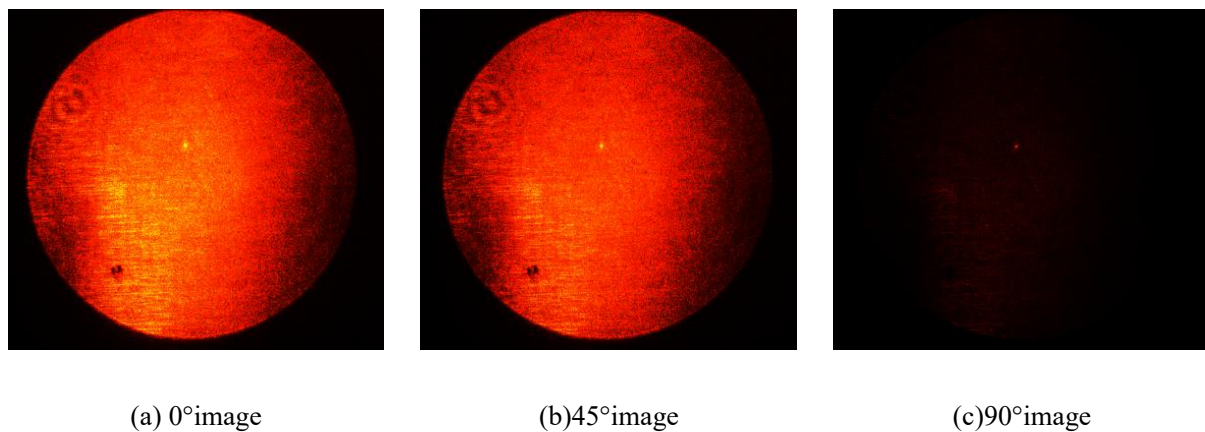


Fig.6 Original polarization image of Zn

The three original images were divided into small areas which the size was 256×256 pixels respectively. And the polarization information of each area was calculated by the Matlab. The obtained polarization degree and polarization angle information were mapped into the HSV color model, then the HSV image corresponding to the material was obtained, as shown in Figure 7.

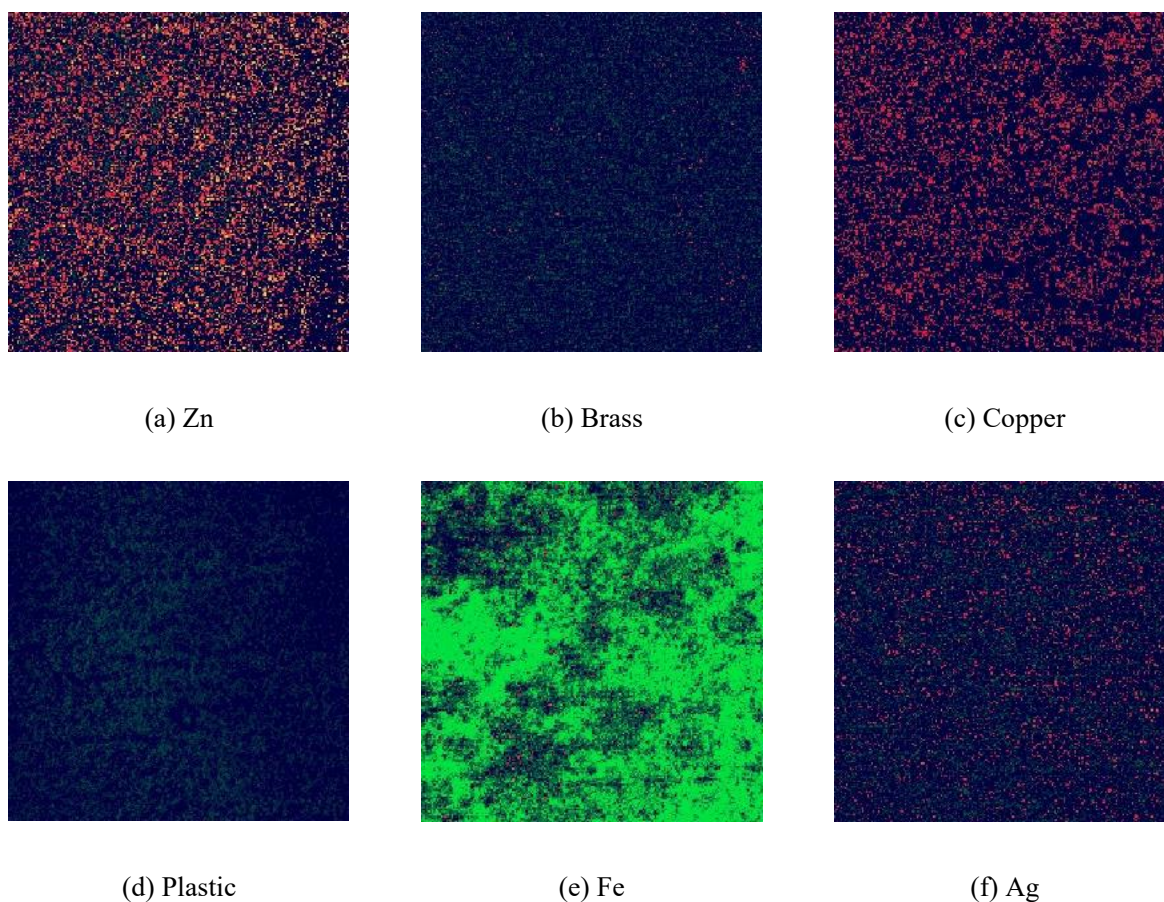


Fig. 7 HSV images of different materials

As can be seen from Figure 7, HSV images of different materials have different colors. But some materials, such as Zn and Copper, have similar HSV images. The difference in HSV color between Fe and other materials is identified easily by human eyes, but not others, for example, the HSV image colors of plastic and brass. Therefore, a CNNs model is needed to identify the Hue and Saturation of the color accurately, so that the material of the target object can be more accurately analyzed.

4. EXPERIMENTAL ENVIRONMENT

The experiment uses the CPU of the workstation to train CNNs with the Caffe framework. The environment parameters of the network model are as follows: the processor is Intel(R) Xeon(R) CPU E5-2630 v4@220GHz (2 processor); the installed memory (RAM) is 64G; The operating system is win10 (64bit); configure Microsoft Visual Studio 2013 software.

5. EXPERIMENTAL RESULTS AND ANALYSIS

The training samples of the experimental network model were the HSV images of brass, copper, Zn, Fe and Ag. Fifty images were obtained for each material and the image size of each type of training sample was 256×256.

In the training process, the total number of iterations was set to 1000, the learning rate was set to 0.001. When the test was repeated 200 times and a network model was generated. For improving the recognition accuracy, some HSV images of various materials were used to test the network, and the training parameters, such as the number of iterations and the learning rate, were adjusted automatically during this step. The loss curve of the model is shown in Fig. 8.

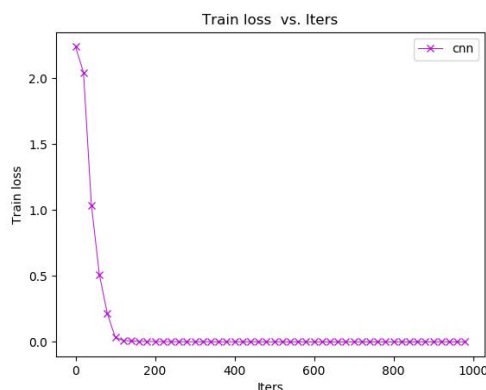


Fig. 8 Loss curve of training CNNs

The simulation results show that the approach of parameter setting by identification and optimization for CNNs is feasible, valid and effective. The value of Loss curve of training CNNs shows "L" form and declines, and then tends to be stable. This phenomenon demonstrates that the design of the model is reasonable. As the number of iterations increases, the error rate of the model recognition gradually close to zero.

In order to check the validity of this method, 50 HSV images of 7 materials were selected for network model testing, and the experiment was repeated 5 times to obtain an average value. The test results are shown in Table 1.

Tab. 1 Network model test results

Object material	brass	copper	Fe	plastic	Zn	Ag	Al
Number of sample	50	50	50	50	50	50	50
Accuracy /%	98	96	98	92	98	98	98

As shown above, the CNNs model can effectively realize the material classification with an accuracy of above 92%. It can meet the most of requirement of computer vision.

6. CONCLUSION

This paper investigated the use of CNNs and polarization imaging technology for material classification. We found that CNNs architectures are capable of learning powerful features from polarization images. With carefully designed pre-training strategies, our method is robust to metal identification with high accuracy.

ACKNOWLEDGEMENTS

The authors acknowledge the supported by the Major Program of the National Natural Science Foundation of China (No.61890964), National Key Research and Development Program Project (No. 2017YFC1404000), National Science and Technology Major Project (No. 2017ZX05019-006), Key Research and Development project of Shandong Province (GG201809250065), Fundamental Research Funds for the Central Universities (No. 19CX05003A-10, No. 18CX02046A).

REFERENCES

- [1] Song W. H., Huo J. R., "Research on computer object recognition based on shape," *Information Technology. Papers* (6):188-190, (2016).
- [2] Fan, Y., Lang , B., "An Object Shape-matching Method Using Contour Orientation Feature," *Computer Technology and Development. Papers* (4):82-86 (2018).

- [3] Zhang H. P., Jiang Z. G., “Multi-view space object recognition and pose estimation based on kernel regression,” Chinese Journal of Aeronautics. Papers 27(05):1233-1241 (2014).
- [4] Han P. L., Liu F., Zhang G., et al, “Multi-scale analysis method of underwater polarization imaging,” Acta Physica Sinica. Papers (5):124-134 (2018).
- [5] Zhou T., Huang D. F., Wang H. M., et al, “Detection Method of Hepatocellular Carcinoma Based on Polarization Properties of Biological Tissue,” Science Technology and Engineering. Papers (7):91-95 (2018).
- [6] Sun Z., Han T. S., Jiang J. Y., et al, “Study on Surface Reflectance Light Elimination of Biological Tissue with Cross-Polarization,” Spectroscopy and Spectral Analysis. Papers (11):3520-3524 (2017).
- [7] Wang X., Zhou X. F., Jin W. Q., “Study of Polarization Properties of Radiation Reflected by Roughness Objects,” Transactions of Beijing Institute of Technology. Papers 31(11):1327-1331 (2011).
- [8] Lu S. J., Li J. Q., Zhang X. L., “Outline Enhancement Technology of Target Based on Polarization Imaging,” Ordnance Industry Automation. Papers (9):66-67,96(2017).
- [9] Li X. L., Li Y. Y., Xie X. H., Xu L. J., "Laser polarization imaging models based on leaf moisture content," Infrared and laser engineering. Papers 46(11):121-126 (2017).
- [10] Peng B., Huang S. L., Li D. J., “Detection of colorless plastic contaminants hidden in cotton layer using chromatic polarization imaging,” Chinese Optics Letters. Papers 13(09):81-85 (2015).
- [11] Cai W. J., Wang L. M., “Recognition of Chinese characters using deep convolutional neural network,” Journal of Image and Graphics. Papers (3):410-417 (2018).
- [12] Lu Z. G., Liu Q. S., Sun Y. B., “Large-Scale Face Image Retrieval based on Deep Residual Embedding Feature,” Journal of Taiyuan University of Technology. Papers (1):106-112 (2018).
- [13] Cai S. Q., “A Study on Rapid Image Super-resolution,” Infrared Technology. Papers (3):269-274 (2018).
- [14] Lu H., Fu X., Liu C., et al, “Cultivated land information extraction in UAV imagery based on deep convolutional neural network and transfer learning,” Journal of Mountain Science. Papers 14(04):731-741 (2017).

- [15] Zhang G. Q., Li Z. M., Li X. W., “Research on color Image segmentation in HSV space,” Computer Engineering and Applications. Papers (26):179-181 (2010).
- [16] Li D. L., Yu Y., Li G. L., et al, “The Study of Underwater Material Recognition Technology,” Laser & Optoelectronics Progress. Papers 55(7):071010 (2018).
- [17] Yin S. H., Deng J. C., Zhang D. W., et al, “Traffic sign recognition based on deep convolutional neural network,” Optoelectronics Letters. Papers 13(06):476-480 (2017).
- [18] Chen H. C., “A Method of vehicle color recognition based on deep convolutional neural networks,” Journal of the Hebei Academy of Sciences. Papers 34(02):1-6 (2017).